Biochimica et Biophysica Acta, 592 (1980) 87—102

BBA 47884

THE ROLE OF MEMBRANE SURFACE CHARGE IN THE CONTROL OF PHOTOSYNTHETIC PROCESSES AND THE INVOLVEMENT OF ELECTROSTATIC SCREENING

B.T. RUBIN and J. BARBER

Botany Department, Imperial College, London S.W.7 (U.K.)

(Received October 29th, 1979)
(Revised manuscript received February 25th, 1980)

Key words: Membrane surface charge; Gouy-Chapman theory; Electrostatic screening; Space charge density; Photosynthesis; (Thylakoid membrane)

Summary

Calculations of changes of the integrated space charge density within the diffuse layer adjacent to a negatively charged membrane surface have been made using analytical expressions derived from the full non-linear Poisson-Boltzmann equation of the Gouy-Chapman theory. This electrostatic screening parameter has been examined for mixed electrolytes of valency type Z^{1+}/Z^{1-} and Z^{2+}/Z^{1-} and concentration ranges were chosen so as to compare with experimental data obtained with thylakoid membranes. The results of the analysis are consistent with previous arguments (Barber, J., Mills, J.D. and Love, A. (1977) FEBS Letts. 74, 174—181) that this screening parameter is involved in the control of salt induced chlorophyll fluorescence and thylakoid stacking changes. Phenomenological equations suggesting the origin of the variations in the integrated space charge density for various salt conditions are presented. Overall the integrated space charge density (σ_x') is shown to be a more satisfactory measure of both short and long range effects associated with electrostatic screening and double layer repulsion of charged surfaces than the planar space charge density (ρ_x).

Introduction

In attempting to explain a number of cation sensitive photosynthetic processes, Barber et al. [1—3] have emphasised the importance of changes in the properties of the electrical diffuse layer adjacent to the negatively charged thylakoid membrane surface [4]. In particular they noted that changes in the positive space charge density within this layer varied in a way which correlated

with known experimental facts while changes in the surface potential did not [1—3]. The experimental observations pertinent to the ideas put forward were the findings that when freshly isolated unwashed thylakoids were suspended in a cation free medium the membranes remained stacked [5], had a maximum fluorescence yield [6], (under conditions when the photosystem II acceptor Q was fully reduced corresponding to the F_m level) and a low 'coupled' rate of electron transport [7]. However, on addition of a low level of monovalent cations (sometimes added with EDTA as a chelating anion [8,9]) the membranes unstacked [5], the maximum fluorescence yield F_m dropped to a lower level [6] and electron transport increased to an uncoupled rate [7]. Restoration of the original state could be accomplished by addition of cations with an effective order of $C^{3+} > C^{2+} > C^{+}$. Although the cation concentration ranges for stacking and fluorescence changes were about the same [2] a lower range was required for the coupling/uncoupling changes in electron transport [7] and also in the latter case special conditions were sometimes necessary for the recoupling process (adding back CF_1 complex; [10]). Nevertheless all three processes share the same characteristics of antagonism between low and high levels of monovalent cations and between low levels of divalent and monovalent cations. Also these phenomena are essentially independent of the anion of the salts used, changes in osmotic strength of the media and of the chemical nature of the cation within a particular valency group * [6].

It was these properties, coupled to the finding that the charge carried by the cations was the dominating factor which prompted Barber and colleagues to realise the importance of electrostatic screening in controlling membrane conformational states manifested by the changes in fluorescence, stacking and electron transport.

Since the publication of the earlier papers outlining these ideas [1—3] several lines of evidence have accumulated in support of the overall concept [4,6,9—13]. For example, according to the theoretical analyses based on the Gouy-Chapman theory, the high level of electrostatic screening which occurs in salt free media was only possible if divalent cations were the dominating charged species in the diffuse layer. It has now been shown experimentally that at the unwashed isolated thylakoid membrane surface, Mg^{2+} is the major cation [10]. However, although the space charge density was emphasised as the screening parameter responsible for membrane conformational changes the treatment given was not rigorous and no explanation was offered for the changes which occurred in this quantity under various salt conditions. Although electrostatic screening or shielding of a charged surface should be defined as the integrated space charge density under a particular electrolyte condition, no such integration was conducted in the earlier analyses. The objective of this paper is to rectify the shortcomings of the previous publications and to discuss in depth the implications of the calculations both in terms of the analytical concepts presented and their consequences in relation to changes in coulombic repulsion between electrically charged surfaces.

---

* This is not true for chemically reactive cations which strongly bind to the membrane surface (see Ref. 14).

Electrical double layer theory

Basic treatment

The Gouy-Chapman theory of the electrical double layer has been extended to mixed electrolytes by Grahame [15]. The application of this theory to thylakoid membranes has been previously discussed [1—3]. For this reason only a brief outline of the theory is now presented and there will be no discussion of the assumptions implicit in its derivations.

For a charged membrane in contact with electrolyte solution containing diffusible ions, the general relation between the electrical potential $\psi_x = \psi(x)$ and the space charge density $\rho_x = \rho(x)$ at a distance x from the membrane surface is given by the Poisson equation:

$$d^2\psi_x/dx^2 = -\rho_x/\epsilon_0\epsilon \tag{1}$$

where ϵ is the dielectric constant of the electrolyte medium (assumed to be independent of changes in the local electric field strength near to the membrane surface) and ϵ_0 is the permittivity of free space. The space charge density at a distance x from the plane of closest approach ($x = 0$) to the membrane surface is determined by the total concentration of ions at x:

$$\rho_x = \sum_i Z_i F C_i(x) \tag{2}$$

where $C_i = C_i(x)$ is the concentration of the ith ion in the plane x, Z_i is the valence of the ith ionic species, F is the Faraday. Under equilibrium conditions, the concentration of species i in the double layer is related to the electrical potential by the Maxwell-Boltzmann law:

$$C_i = C_i^0 e^{-Z_i F\psi_x/RT} \tag{3}$$

where C_i^0 is the bulk concentration of species i, R is the molar gas constant; T is the thermodynamic temperature. Combination of Eqns. 2 and 3 leads to the expression:

$$\rho_x = \sum_i Z_i F C_i^0 e^{-Z_i F\psi_x/RT} \tag{4}$$

Substituting Eqn. 4 into Eqn. 1 yields the usual Poisson-Boltzmann expression:

$$d^2\psi_x/dx^2 = -(1/\epsilon_0\epsilon) \sum_i Z_i F C_i^0 e^{-Z_i F\psi_x/RT} \tag{5}$$

Eqn. 5 may be integrated once when it is assumed that $d\psi_x/dx \to 0$ as $x \to \infty$ to give the electrical field:

$$d\psi_x/dx = \mp \left[(2RT/\epsilon_0\epsilon) \sum_i C_i^0 (e^{-Z_i F\psi_x/RT} - 1)\right]^{1/2} \tag{6}$$

The electric induction at the distance of closest approach to the membrane surface is due to the surface charge density σ_m:

$$\sigma_m = -\epsilon_0\epsilon (d\psi_x/dx)_{x=0} \tag{7}$$

Utilizing Eqn. 6, Eqn. 7 becomes:

$$\sigma_m = \mp \left[(2RT\epsilon_0\epsilon) \sum_i C_i^0 (e^{-Z_i F\psi_0/RT} - 1) \right]^{1/2} \quad (8)$$

where ψ_0 is the electrical potential at the surface plane $x = 0$.

Screening parameter

As explained in the introduction the role of the electrical double layer in controlling chlorophyll fluorescence, thylakoid stacking and electron transport depends in part on the extent to which the membrane surface charges are shielded by cations in the surrounding medium. A measure of the screening capacity of a given mixed electrolyte medium to shield the charge on a membrane surface is the integrated space charge density and its variation with distance:

$$\sigma_x' = -\int_{x=0}^{x} \frac{\rho_x \, dx}{\sigma_m} \quad (9)$$

where σ_x' is the integrated space charge density up to plane x normalised by the membrane surface charge density σ_m. If σ_m is assumed constant then,

$$\sigma_x' = -(1/\sigma_m) \int_{x=0}^{x} \rho_x \, dx \quad (10)$$

Employing Eqns. 1 and 7, Eqn. 10 is transformed to read:

$$\sigma_x' = 1 - (d\psi_x/dx)/(d\psi_x/dx)_{x=0} \quad (11)$$

Eqn. 11 satisfies the condition that as $x \to \infty$, $(d\psi_x/dx) \to 0$ whence $\sigma_x' \to 1$.

In the case of an assymetric mixed electrolyte system of valence type: (Z^{1+}/Z^{1-}, Z^{2+}/Z^{1-}) such as (KCl, $MgCl_2$) in contact with a negatively charged membrane surface, equation (6) may be integrated analytically by introducing the parameter ν (see Acknowledgements) as shown in Appendix A

$$\kappa x = \tanh^{-1}(\nu/\sqrt{\gamma}) - \phi_0 \quad (12)$$

where

$$\nu = [C_2^0 + (C_1^0 + 2C_2^0) e^{-F\bar{\psi}_x/RT}]^{1/2} \quad (13)$$

$$\gamma = (C_1^0 + 3C_2^0) \quad (14)$$

$$\phi_0 = \tanh^{-1}(\nu_0/\sqrt{\gamma}) \quad (15)$$

$$\kappa = (F^2\gamma/2\,RT\epsilon_0\epsilon)^{1/2} \quad (16)$$

whilst $\bar{\psi}_x = |\psi_x|$ and ν_0 is the value of ν when $\bar{\psi}_x = \bar{\psi}_0$. Here C_1^0, C_2^0 are the bulk concentrations of monovalent and divalent cationic species respectively. From Eqn. 12 the potential may be written as (see Appendix A)

$$-\bar{\psi}_x = (RT/F) \ln\{ [\gamma \tanh^2(\phi_0 + \kappa x) - C_2^0]/(C_1^0 + 2C_2^0)\} \quad (17)$$

The corresponding electric field may be written as:

$$-d\bar{\psi}_x/dx = (2RT\gamma^2/\epsilon_0\epsilon)^{1/2} [\nu/(\nu^2 - C_2^0)] \operatorname{sech}^2(\phi_0 + \kappa x) \quad (18)$$

Employing Eqn. 18, the screening parameter σ'_x defined by Eqn. 11 becomes:

$$\sigma'_x = 1 - \frac{[\nu/(\nu^2 - C_2^0)]\ \mathrm{sech}^2(\phi_0 + \kappa x)}{[\nu_0/(\nu_0^2 - C_2^0)]\ \mathrm{sech}^2(\phi_0)} \tag{19}$$

Calculations on the assymetric mixed electrolyte system of valence type $(Z^{1+}/Z^{1-}, Z^{2+}/Z^{1-})$

Computation procedure

Assuming constant values of the parameters $\sigma_m = -2.5 \cdot 10^{-2}$ C/m^2, $\epsilon = 78.4$, $T = 298.16$ K the surface potential ψ_0 was calculated from Eqn. 8 over a range of monovalent cation concentrations for various fixed background values of divalent cation concentrations. For a given ψ_0 and fixed salt condition $\bar{\psi}_x$ was evaluated at different values of x using Eqn. 17. The corresponding values of the electric field at each distance x were calculated from Eqn. 18 with the use of Eqn. 13. The space charge density at a given distance x was calculated using Eqn. 4 with the corresponding value of $\bar{\psi}_x$ previously evaluated. The integrated space charge density σ'_x was calculated at different values of x from Eqn. 19 with the use of Eqn. 13. The calculation procedure was repeated for a range of divalent cation concentrations for various fixed background values of monovalent cation concentrations. The electrolyte concentrations adopted in the calculations were chosen to be in the range of those used by experimenters and known to induce the various salt induced phenomena outlined in the introduction. The value of the surface charge density is the same as that used previously [1—3] and shown to be acceptable for the thylakoids as estimated from experimental measurements [4,13,14].

Results

In Fig. 1 computer derived curves show changes in (a) the surface potential ψ_0, (b) the space charge density ρ_x at one background divalent cation concentration at different distances from the membrane surface, (c) the corresponding integrated space charge density σ'_x under identical salt conditions at difference distances from the membrane surface, and (d) the integrated space charge density σ'_x at various fixed background divalent cation concentrations as a function of the monovalent cation concentration level. Fig. 2 depicts analogous curves for ψ_0, ρ_x, σ'_x at various background monovalent cation concentrations as a function of the divalent cation concentration level.

Fig. 1b manifests a minimum or 'dip' in the space charge density ρ_x in the monovalent cation concentration range $1.0 < C_1^0 < 10$ mM for a fixed divalent cation background concentration of $C_2^0 = 10^{-3}$ mM. The occurrence of the 'dip' penetrates out to a distance $x \leqslant 1.0$ nm.

Fig. 1c indicates that for the same salt conditions as in Fig. 1b the integrated space charge density σ'_x exhibits a minimum or 'dip' which persists out to a distance of $x \geqslant 10.0$ nm. The relative depth of the 'dip' measured at a given x may be defined as:

$$\Delta\sigma'_x = \sigma'_{xs}(C_{1s}^0, C_2^0, x) - \sigma'_x(C_1^*, C_2^0, x) \tag{20}$$

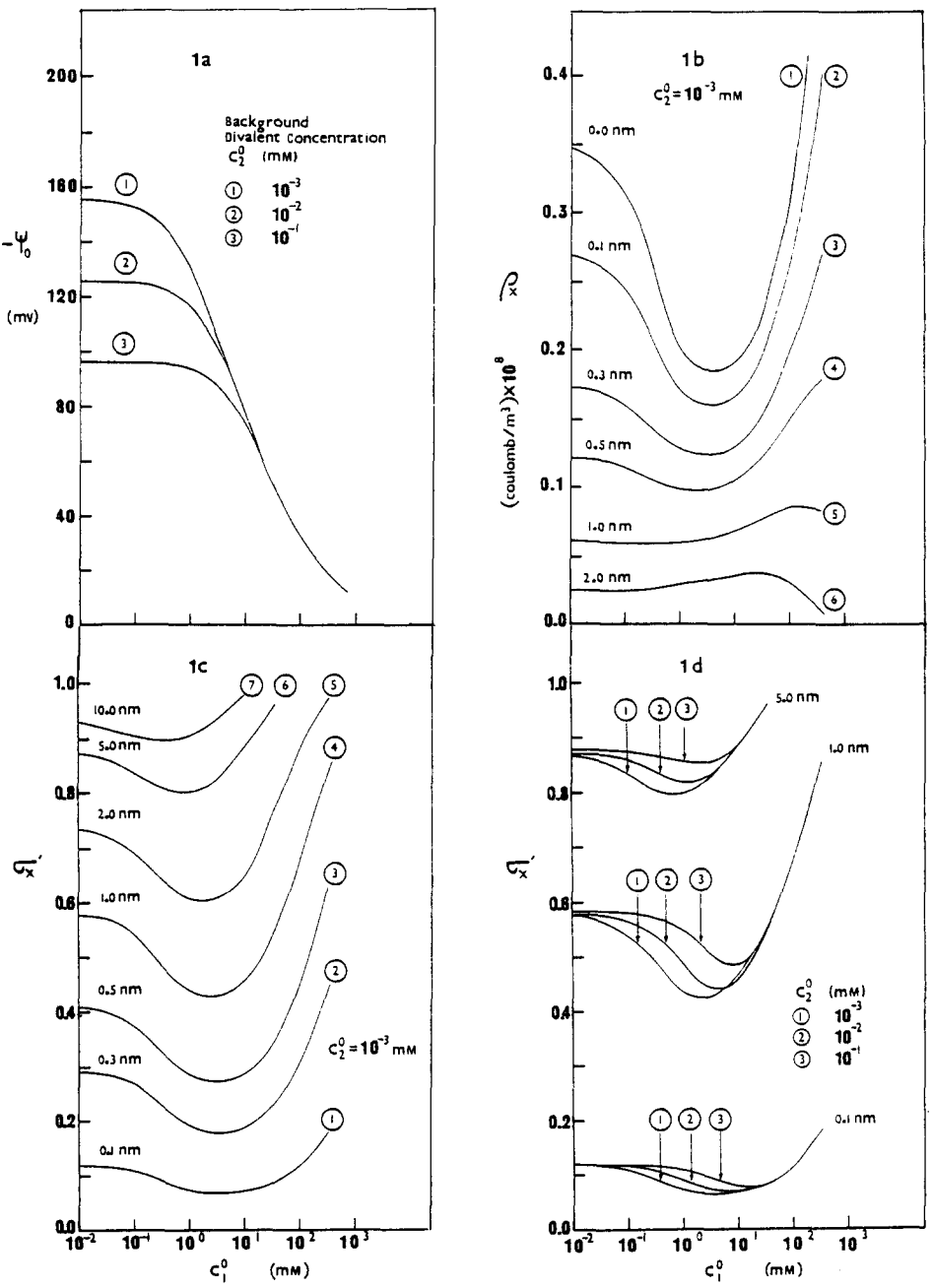

Fig. 1. Computer derived curves showing changes in (a) the surface potential ψ_0 at three fixed background divalent cation concentrations C_2^0, (b) the space charge density ρ_x at different distances from the membrane surface at one fixed background divalent cation concentration C_2^0, (c) the corresponding integrated space charge density σ_x' at different distances from the membrane surface under identical salt conditions as (b), and (d) the integrated space charge density σ_x' for three distances from the membrane surface at three fixed background divalent cation concentrations C_2^0 shown as a function of monovalent cation concentration level C_1^0 in the mixed electrolyte solution of valence type: (Z^{1+}/Z^{1-}, Z^{2+}/Z^{1-}).

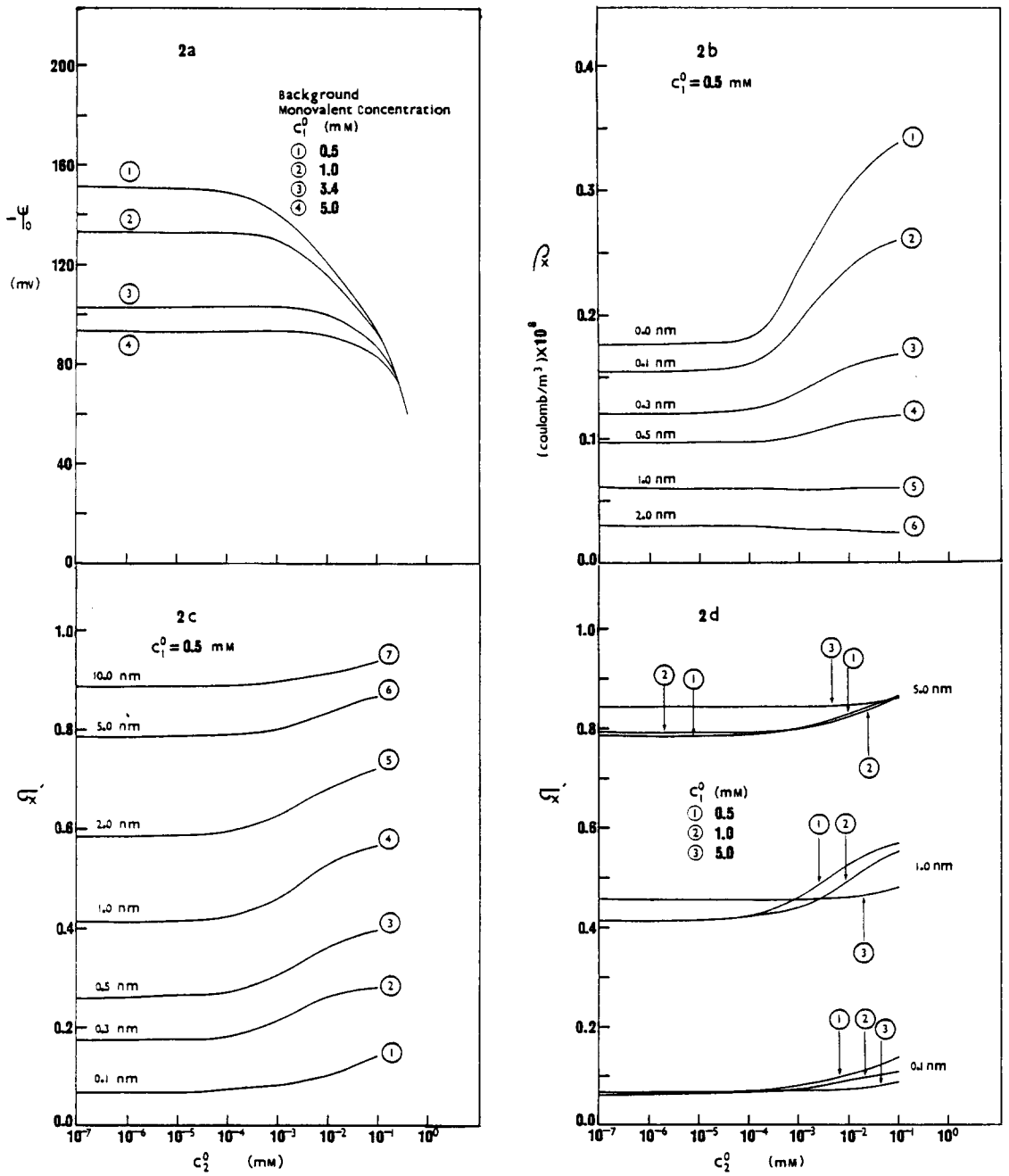

Fig. 2. Computer derived curves showing changes in (a) surface potential ψ_0 at four fixed background monovalent cation concentrations C_1^0, (b) the space charge density ρ_x at different distances from the membrane surface at one fixed background monovalent cation concentration C_1^0, (c) the corresponding integrated space charge density σ_x' at different distances from the membrane surface under identical salt conditions as (b), and (d) the integrated space charge density σ_x' for three distances from the membrane surface at three fixed background monovalent cation concentrations C_1^0 shown as a function of the divalent cation concentration level C_2^0 in the mixed electrolyte solution of valence type: (Z^{1+}/Z^{1-}, Z^{2+}/Z^{1-}).

where σ'_{xs} is the integrated space charge density referred to an arbitrary standard initial monovalent cation concentration $C_1^0 = C_{1s}^0 = 10^{-2}$ mM; C_1^* is the 'critical' monovalent cation concentration at which the 'dip' effect occurs. From Fig. 1c a maximum in $\Delta\sigma'_x$ is apparent at $x = x^* \cong 1.0$ nm. Further the 'dip' shifts to lower critical monovalent cation concentrations with increasing distance from the membrane surface. The shift in C_1^* over a distance of $x = 10.0$ nm corresponds approximately to one decade change in monovalent cation concentration.

Fig. 1d demonstrates the relative shift of the 'dip' in the integrated space charge density to higher critical monovalent cation concentrations with increasing background level of divalent cation concentration at three distances from the membrane surface. Also, with increasing background divalent cation levels the depth of the 'dip' is reduced.

It is apparent in both Figs. 1c and 1d that for a fixed background divalent cation concentration level and a fixed value of C_1^0 along the monovalent cation concentration axis that $\sigma'_x \to 1$ as $x \to \infty$.

In Fig. 2b no significant minimum or 'dip' in the space charge density ρ_x is apparent as a function of divalent cation concentration level over the range $10^{-7} \leqslant C_2^0 \leqslant 10^{-1}$ mM and a fixed background monovalent cation concentration of $C_1^0 = 0.5$ mM.

In Fig. 2c no 'dip' in the integrated space charge density σ'_x is apparent under identical salt conditions investigated as in Fig. 2b.

Similarly, Fig. 2d evidences no 'dip' effect in σ'_x over the range of salt conditions examined: $10^{-7} \leqslant C_2^0 \leqslant 10^{-1}$ mM in divalent cation concentration levels and $0.5 \leqslant C_1^0 \leqslant 5.0$ mM in fixed background monovalent cation concentration levels for three distances from the membrane surface. However, it should be noted in Fig. 2d that increasing the background monovalent cations resulted in the necessity to add higher levels of divalent cations to bring about an increase in space charge density integrated out to a distance of 1 nm.

The criterion implicit in a valid comparison of Figs. 1 and 2 rests on the choice of a similar surface potential range as is shown in Figs. 1a and 2a.

Discussion

Origin of 'dip' effect

For a mixed electrolyte system of valence type: (Z^{1+}/Z^{1-}, Z^{2+}/Z^{1-}) in contact with a negatively charged membrane surface, $\sigma_m > 0$ and $\psi_x < 0$. The space charge density at any distance x from the surface is given by Eqn. 4 in Basic treatment, i.e.

$$\rho(x) = FC_1^0(e^y - e^{-y}) + 2FC_2^0(e^{2y} - e^{-y}) \tag{21}$$

where

$$y(x) = F|\psi(x)|/RT \tag{22}$$

The variation of ρ with monovalent cation concentration level C_1^0 at a fixed background divalent cation concentration level C_2^0 is

$$(d\rho/dC_1^0)_{C_2^0} = (\partial\rho/\partial C_1^0)_{C_{2,y}^0} + (\partial\rho/\partial y)_{C_1^0, C_2^0}\, dy/dC_1^0 \tag{23}$$

For a minimum 'dip' to occur:

$$(d\rho/dC_1^0)_{C_2^0} = 0 \quad \text{when } C_1^0 = C_1^* \tag{24}$$

Thus, at the critical concentration C_1^* the two terms on the right hand side of Eqn. 23 must sum to zero. Consequently,

$$(dy/dC_1^0)_{C_1^0 = C_1^*} = -\left[\frac{(\partial\rho/\partial C_1^0)_{C_{2,y}^0}}{(\partial\rho/\partial y)_{C_1^0, C_2^0}}\right]_{C_1^0 = C_1^*} \tag{25}$$

Eqn. 25 is required for numerical comparison in the following section.

The variation of ρ with divalent concentration levels at a fixed background monovalent cation concentration level is

$$(d\rho/dC_2^0)_{C_1^0} = (\partial\rho/\partial C_2^0)_{C_{1,y}^0} + (\partial\rho/\partial y)_{C_1^0, C_2^0}\, dy/dC_2^0 \tag{26}$$

Substituting Eqn. 21 into Eqns. 23 and 26 respectively obtains:

$$(d\rho/dC_1^0)_{C_2^0} = F(e^y - e^{-y}) + \lambda\, dy/dC_1^0 \tag{27}$$

$$(d\rho/dC_2^0)_{C_1^0} = 2F(e^{2y} - e^{-y}) + \lambda\, dy/dC_2^0 \tag{28}$$

where:

$$\lambda = FC_1^0(e^y + e^{-y}) + 2FC_2^0(2e^{2y} + e^{-y}) \tag{29}$$

In order to compare Eqns. 27 and 28 we restrict the analysis to the plane $x = 0$ such that $y = y_0 = F|\psi_0|/RT$ by Eqn. 22. From Fig. 1b the predominant 'dip' in ρ occurs at the plane $x = 0$. The critical monovalent cation concentration is $C_1^* = 3.4$ mM. The corresponding surface potential at the same background divalent cation concentration $C_2^0 = 10^{-3}$ mM is found from Fig. 1a curve (1) as $|\psi_0| \cong 103$ mV. Substituting Eqn. 21 into Eqn. 25 and employing the values of $|\psi_0|$, C_1^*, C_2^0, the term (dy/dC_1^0) is calculated as -0.276. Under the same conditions the term (dy/dC_2^0) is evaluated from Fig. 2a curve 3 as approx. -20.00. Eqn. 27 under the restrictions of the calculations requires $(d\rho/dC_1^0)_{C_2^0} = 0$, whereas Eqn. 28 yields the result $(d\rho/dC_2)_{C_1^0} \cong 2.01 \cdot 10^8$. Clearly, $(d\rho/dC_2^0)_{C_1^0} > 0$. Thus, the dominant effect of the valence in the leading exponential term in Eqn. 28, e^{2y}, combines with the relatively smaller value of the term $\lambda(dy/dC_2^0)_{C_1^0}$ to obtain: $(d\rho/dC_2^0)_{C_1^0} > 0$. Hence, no significant 'dip' in the space charge density is evident over these electrolyte conditions. In contrast Eqn. 27 reveals that the effect of a lower valence in the leading exponential term, e^y, produces a leading term whose value is equal and opposite in sign to the term $\lambda(dy/dC_1^0)$ thus generating a minimum in the space charge density for the given range of salt conditions explored. The corresponding integrated space charge density exhibits similar behaviour with respect to the occurrance of a minimum. The effect of integration of the space charge density is to extend the occurrance of the minimum to distances further away from the membrane surface.

Variation of depth of the 'dip' in the integrated space charge density and shift of the 'dip' with distance from the membrane surface

The variation of the relative depth of 'dip' in the integrated space charge density with distance for a specified set of salt conditions (see Fig. 1c) may be examined by considering the parameter $\Delta\sigma'_x$ defined by Eqn. 20 in Results. The variation in $\Delta\sigma'_x$ with distance is

$$\frac{d\Delta\sigma'_x}{dx} = \frac{d}{dx}\left[\sigma'_{xs}(C^0_{1s}, C^0_2, x) - \sigma'_x(C^*_1, C^0_2, x)\right] \tag{30}$$

where C^0_{1s} was arbitrarily chosen as 10^{-2} mM to be the standard initial value along the monovalent cation concentration axis to which σ'_{xs} is referred. Expanding Eqn. 30 maintaining C^0_{1s}, C^0_2 fixed obtains

$$\frac{d\Delta\sigma'_x}{dx} = \left(\frac{\partial\sigma'_{xs}}{\partial x}\right)_{C^0_{1s},C^0_2} - \left(\frac{\partial\sigma'_x}{\partial x}\right)_{C^*_1,C^0_1} - \left(\frac{\partial\sigma'_x}{\partial C^*}\right)_{C^0_2,x}\frac{dC^*_1}{dx} \tag{31}$$

Using Eqn. 10 in *Screening Parameter*, Eqn. 31 becomes:

$$\frac{d\Delta\sigma'_x}{dx} = (\rho^s - \rho^*)/\sigma_m - \left(\frac{\partial\sigma'_x}{\partial C^*_1}\right)_{C^0_2,x}\frac{dC^*_1}{dx} \tag{32}$$

where ρ^s is the space charge density referred to the standard initial concentration C^0_{1s} and ρ^* is the space charge density referred to the critical monovalent concentration C^*_1. Fig. 1c indicates a maximum in $\Delta\sigma'_x$ at $x = x^* \cong 1.0$ nm, i.e.

$$\left[\frac{d\Delta\sigma'_x}{dx}\right]_{x=x^*} = 0\,. \tag{33}$$

Consequently,

$$[(\rho^s - \rho^*)/\sigma_m]_{x=x^*} = \left(\frac{\partial\sigma'_x}{\partial C^*_1}\right)_{C^0_2,x=x^*} \times \left(\frac{dC^*_1}{dx}\right)_{x=x^*} \tag{34}$$

Eqn. 34 states that a maximum in the depth of the dip occurs at a given distance $x = x^*$ when the difference in space charge density exactly balances the product of the variation of integrated space charge density with critical monovalent cation concentration and the variation of critical monovalent cation concentration with distance. The term (dC^*_1/dx) in Eqn. 32 accounts for the observed shift in the 'dip' to lower critical monovalent cation concentrations with increasing distance from the membrane surface.

Shift in the 'dip' of the integrated space charge density with background divalent cation concentration

The relative shift in C^*_1 to higher critical monovalent cation concentrations with increasing background level of divalent cation concentration at a given fixed distance from the membrane surface (see Fig. 1d) is derived as follows. The variation of the parameter $\Delta\sigma'_x$ with divalent cation concentration level is:

$$\frac{d\Delta\sigma'_x}{dC^0_2} = \frac{d}{dC^0_2}\left[\sigma'_{xs}(C^0_{1s}, C^0_2, x) - \sigma'_x(C^*_1, C^0_2, x)\right] \tag{35}$$

Expanding Eqn. 35 maintaining C^0_{1s}, x, fixed and rearranging the terms yields the desired relation:

$$\left(\frac{dC_1^*}{dC_2^0}\right) = \frac{\left(\frac{\partial \sigma'_{xs}}{\partial C_2^0}\right)_{C^0_{1s},x} - \left(\frac{\partial \sigma'_x}{\partial C_2^0}\right)_x - \left(\frac{d\Delta\sigma'_x}{dC_2^0}\right)_x}{\left(\frac{\partial \sigma'_x}{\partial C_1^*}\right)_x} \tag{36}$$

Eqn. 36 describes the variation in the critical monovalent cation concentration with background divalent cation concentration levels as a complicated function of several terms. Thus this expression can be used to calculate the shift in the critical monovalent cation concentration as a function of background divalent cation levels at a fixed distance from the membrane surface.

Relevance of the integrated space charge density

The spatial relationship between two electrically charged surfaces immersed in electrolyte solution is determined in the simplest case by a balance between hydrodynamic forces, Van der Waals attractive forces, and coulombic double layer repulsive forces. The formal connection between the integrated space charge density σ'_x and the double layer repulsive force π arising from the interaction of two parallel charged place surfaces is derived in Appendix B, i.e.:

$$\pi = (p_i - p_e) - \tfrac{1}{2}[(2\epsilon_0\epsilon_i - \epsilon_0)\{E_x/(1-\sigma'_x)\}^2_I - (2\epsilon_0\epsilon_e - \epsilon_0)\{E_x/(1-\sigma'_x)\}^2_{II}] \tag{37}$$

where (p_i, p_e), (ϵ_i, ϵ_e) are the Kelvin pressures and the dielectric constants respectively in the electrolyte fluid in contact with the internal (i) and external (e) faces of the place surfaces (Refer to Fig. 3). The quantities $\{E_x/(1-\sigma'_x)\}_I$, $\{E_x/(1-\sigma'_x)\}_{II}$ are the electric fields (E_i, E_e) respectively acting at the internal and external faces of the membrane plate surface. Subscripts I and II denote

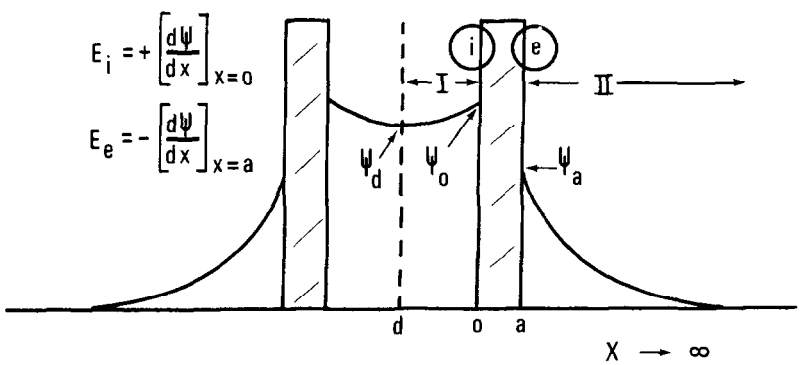

Fig. 3. Model for the calculation of the double layer repulsive force between two parallel charged plate surfaces immersed in electrolyte medium. Hatched areas represent the plates. The interplate region I is defined in the domain: $d < x \leqslant 0$; the outerplate region II is defined in the domain: $a \leqslant x < \infty$. E_i, E_e are the electric fields acting at the internal (i) and external (e) faces respectively of the plate surface. The midplane potential ψ_d, and the surface potentials ψ_0, ψ_a are shown on the potential profile.

interplate and outerplate regions respectively and E_x is defined as $E_x = -d\psi_x/dx$. A knowledge of σ'_x and E_x at any distance x in the domain of a given region determines the corresponding value of the electric field at the plate surface. A reduction in the quantity $\{E_x/(1-\sigma'_x)\}_I$ relative to the quantity $\{E_x/(1-\sigma'_x)\}_{II}$ is expected to generate an increase in the repulsive force π. Thus, an increase in the repulsive force π may result from a relative decrease in σ'_x in region I compared with region II and is thought to occur when thylakoid membranes are suspended in low salt media and have monovalent cations as the major counter-ion at their surfaces. It is noteworthy to point out that a 5% change in the quantity $\{E_x/(1-\sigma'_x)\}$ introduces an approximately 10% change in the quantity $\{E_x/(1-\sigma'_x)\}^2$ suggesting that a relatively modest variation in the integrated space charge density may introduce a significantly greater variation in the repulsive force. The notion that the double layer repulsive force may be controlled by varying the electrolyte composition is well established in colloid science [16] and is clearly expressed in the stacking and unstacking behaviour of the thylakoid membranes [2]. In this regard the calculation of forces between charged membrane surfaces are particularly relevant [17,18].

The interesting finding that electrostatic screening of surface negative charges can be high even in essentially salt free media is demonstrated theoretically and experimentally when divalent cations are the only species in the diffuse layer [2,5,13,19]. In contrast, when monovalent cations are in the diffuse layer under very low salt conditions the screening parameter σ'_x has a lower value within the majority of the diffuse double layer as shown by comparing Fig. 1c with Fig. 2c at the same distance from the membrane surface, and by the fact that the thylakoids are unstacked in this condition [2,5,13, 19]. Similar behaviour to salt induced thylakoid stacking changes has been observed in salt induced coagulation-repeptization phenomena occurring in negatively charged AgI sol under mixed monovalent and divalent electrolyte conditions [20].

In applying the idea that the integrated space charge density is a measure of both the screening capacity of an electrolyte medium to shield charge on a membrane surface and of the repulsive interaction between charged surfaces, it should be recognized that biological membranes are not rigid nor homogeneous. They usually consist of large protein complexes embedded in a lipid matrix often having additional extrinsic proteins absorbed on their surface. In addition to contributing to the coulombic repulsion between membrane surfaces, the integrated space charge density in a lamina near the surface is expected to affect the interactions between surfaces of exposed portions of intrinsic protein complexes as well as interactions between the membrane and the charged surface of extrinsic proteins. The integrated space charge density thus exhibits both short and long range effects whereas the space charge density displays essentially short range effects. As seen from Figs. 1b and 1c the penetration of the 'dip' effect in ρ_x extends out to distances of $x \leqslant 1.0$ nm whereas the 'dip' effect in σ'_x persists out to distances $x \geqslant 10.0$ nm. It is the recognition of both the short and long range nature of the interactions that has given rise to an explanation for the inter-relationship between thylakoid stacking and chlorophyll fluorescence changes [21] and for the binding of the CF_1 portion of the coupling factor to the thylakoid surface [9] also

observed as changes in the rate of electron transport [8,9]. In the case of the thylakoid stacking and associated chlorophyll fluorescence changes, it has been argued that a change from poor to good electrostatic screening results in lateral diffusion of chlorophyll-protein complexes in such a way as to decrease energy transfer (observed as an increase in chlorophyll fluorescence) and create heterogeneity in the distribution of surface charge so as to account for the formation of granal (stacked) and stromal (unstacked) membranes [6,13,21].

Finally it should be mentioned that the effect of different background levels of divalent cations on the ability of monovalent cations to decrease the integrated space charge density (Fig. 1d) and the effect of different low background levels of monovalent cations on the ability of divalent cations to increase the screening parameter (Fig. 2d) is consistent with experimental evidence [1—3,7,22].

Concluding remarks

The effects of screening in the electrical double layer have been examined in the mixed electrolyte system of valence type: Z^{2+}/Z^{1-}, Z^{2+}/Z^{1-}). Phenomenological equations suggesting the origin of the 'dip' in screening and shifts in this minimum under various electrolyte conditions have been proposed. The outcome of the analysis is consistent with the previous arguments that the positive space charge density close to the thylakoid surface is the electrical parameter involved in salt induced membrane phenomena. However, the use of the integrated space charge density parameter is far more satisfactory since it reflects both the short and long range nature of salt induced membrane conformational changes associated with thylakoid stacking, chlorophyll fluorescence and electron transport.

Clearly, the idea that changes in the integrated space charge density can bring about changes in the balance of forces between charged surfaces is applicable not only to the phenomena mentioned but also to other processes which involve the interaction between intrinsic membrane proteins and between extrinsic proteins and their functional sites on the membrane surfaces. Therefore the above analyses should be of interest to others who are studying the effects of various salt treatments on enzymic and membrane controlled processes which are likely to involve electrostatic interactions.

Appendix A

Derivation of the potential, electric field and integrated space charge density via the parameter ν. The electric field given by expression 6 in Basic treatment of the text is

$$d\psi_x/dx = \mp[(2RT/\epsilon_0\epsilon) \sum_i C_i^0(e^{-Z_iF\psi_x/RT} - 1)]^{1/2} \qquad A(1)$$

The integral representation of A(1) is

$$x = \mp(\epsilon_0\epsilon/RT)^{1/2} \int_{\psi_0}^{\psi_x} d\psi_x \Big/ \left[\sum_i C_i^0(e^{-Z_iF\psi_x/RT} - 1)\right]^{1/2} \qquad A(2)$$

For an electrolyte mixture of valence type: (Z^{1+}/Z^{1-}, Z^{2+}/Z^{1-}) in contact with a negatively charged surface: $\sigma_m < 0$, $\psi_x < 0$. The term involving the sum is then:

$$\sum_i C_i^0 (e^{Z_i F\bar{\psi}_x/RT} - 1) = (C_1^0 + 2C_2^0)\, e^{-F\bar{\psi}_x/RT} + C_1^0 e^{F\bar{\psi}_x/RT} + C_2^0 e^{2F\bar{\psi}_x/RT} - (2C_1^0 + 3C_2^0) \quad \text{A(3)}$$

where:

$$\bar{\psi}_x = |\psi_x| \quad \text{A(4)}$$

Define a parameter ν (see Acknowledgement) such that:

$$\nu = [C_2^0 + (C_1^0 + 2C_2^0)\, e^{-F\bar{\psi}_x/RT}]^{1/2} \quad \text{A(5)}$$

$$d\nu = -(F/2RT)\,[(\nu^2 - C_2^0)/\nu]\, d\bar{\psi}_x \quad \text{A(6)}$$

From A(5)

$$e^{F\bar{\psi}_x/RT} = (C_1^0 + 2C_2^0)/(\nu^2 - C_2^0) \quad \text{A(7)}$$

Substituting A(5) and A(7) into A(3) obtains:

$$\sum_i C_i^0 (e^{Z_i F\bar{\psi}_x/RT} - 1) = [\nu^2/(\nu^2 - C_2^0)^2][\nu^2 - \gamma]^2 \quad \text{A(8)}$$

where:

$$\gamma = (C_1^0 + 3C_2^0) \quad \text{A(9)}$$

Substituting A(8) into A(2) and employing A(6) noting that $d\psi_x \to -d|\psi_x|$ eqn. A(2) reduces to:

$$x = (2RT\epsilon_0\epsilon/F^2)^{1/2} \int_{\nu_0}^{\nu} d\nu/[(\sqrt{\gamma})^2 - \nu^2] \quad \text{A(10)}$$

where the negative sign preceding the right hand side of Eqn. A(2) has been taken in this case. Eqn. A(10) may be integrated to obtain:

$$\kappa x = \tanh^{-1}(\nu/\sqrt{\gamma}) - \phi_0 \quad \text{A(11)}$$

where

$$\kappa = (F^2\gamma/2RT\epsilon_0\epsilon)^{1/2} \quad \text{A(12)}$$

$$\phi_0 = \tanh^{-1}(\nu_0/\sqrt{\gamma}) \quad \text{A(13)}$$

$$\nu_0 = [C_2^0 + (C_1^0 + 2C_2^0)\, e^{-F\bar{\psi}_0/RT}]^{1/2} \quad \text{A(14)}$$

Solving A(11) for ν gives

$$\nu = \sqrt{\gamma}\,\tanh(\phi_0 + \kappa x) \quad \text{A(15)}$$

Squaring Eqn. A(15), introducing A(5) and solving for the potential $-\bar{\psi}_x$ gives:

$$-\bar{\psi}_x = (RT/F)\ln\{[\gamma \tanh^2(\phi_0 + \kappa x) - C_2^0]/(C_1^0 + 2C_2^0)\} \quad \text{A(16)}$$

A convenient expression for the electric field may be obtained by differentiat-

ing A(15) with respect to x and introducing A(6) gives:

$$-d\bar{\psi}_x/dx = (2RT\gamma^2/\epsilon_0\epsilon)^{1/2}[\nu/(\nu^2 - C_2^0)]\ \mathrm{sech}^2(\phi_0 + \kappa x) \qquad \text{A(17)}$$

Employing A(17), the screening parameter given by eqn. 11:

$$\sigma_x' = 1 - (d\psi_x/dx)/(d\psi_x/dx)_{x=0} \qquad \text{A(18)}$$

becomes:

$$\sigma_x' = 1 - \frac{[\nu/(\nu^2 - C_2^0)]\ \mathrm{sech}^2(\phi_0 + \kappa x)}{[\nu_0/(\nu_0^2 - C_2^0)]\ \mathrm{sech}^2(\phi_0)} \qquad \text{A(19)}$$

For calculation purposes Eqn. A(13) may be written as

$$\phi_0 = \tanh^{-1}(\nu_0/\sqrt{\gamma}) = \tfrac{1}{2}\ln\left\{\left|\frac{1 + \nu_0/\sqrt{\gamma}}{1 - \nu_0/\sqrt{\gamma}}\right|\right\} \qquad \text{A(20)}$$

Appendix B

The double layer repulsion between two parallel charged plates immersed in electrolyte solution is given by the Verwey-Overbeek equation [23]:

$$\pi = p_d - p_\infty \qquad \text{B(1)}$$

where π is the repulsive force in the external direction (per unit area of external face of the plate), p_d is the hydrostatic pressure at the middle of the interplate region, p_∞ is the hydrostatic pressure in the fluid far from the plates where the electric field is zero. As discussed by Sanfeld [24], p_d and p_∞ may be expressed in terms of the electric fields (E_i, E_e), dielectric constants (ϵ_i, ϵ_e), and the Kelvin pressures (p_i, p_e) in the fluid in contact with the internal (i) and external (e) faces of the plate surfaces respectively, (refer to Fig. 3) i.e.

$$p_d = p_i - \tfrac{1}{2}(2\epsilon_0\epsilon_i - \epsilon_0)E_i^2 \qquad \text{B(2)}$$

$$p_\infty = p_e - \tfrac{1}{2}(2\epsilon_0\epsilon_e - \epsilon_0)E_e^2 \qquad \text{B(3)}$$

Here ϵ_0 is the permittivity of free space. Eqn. B(1) is then written as:

$$\pi = (p_i - p_e) - \tfrac{1}{2}[(2\epsilon_0\epsilon_i - \epsilon_0)E_i^2 - (2\epsilon_0\epsilon_e - \epsilon_0)E_e^2] \qquad \text{B(4)}$$

The electric fields E_i, E_e may be formally expressed in terms of the integrated space charge density σ_x' by applying Eqn. 11 in the text, i.e.

$$E_i = \{E_x/(1 - \sigma_x')\}_I \qquad d < x \leqslant 0 \qquad \text{B(5)}$$

$$E_e = \{E_x/(1 - \sigma_x')\}_{II} \qquad a \leqslant x < \infty \qquad \text{B(6)}$$

where we have used the definition $E = -d\psi/dx$. Subscript I denotes the interplate region bounded by the midplane and the internal face of the plate surface; subscript II denotes the outer plate region bounded by the external face of the plate surface and a plane in the bulk fluid corresponding to zero electric field. Eqns. B(5) and B(6) indicate that a knowledge of E_x and $(1 - \sigma_x')$ at any x in a given region determine the corresponding value of the electric field at the

plate surface. Substituting B(5) and B(6) into B(4) gives the desired relation:

$$\pi = (p_i - p_e) - \tfrac{1}{2}[(2\epsilon_0\epsilon_i - \epsilon_0)\{E_x/(1-\sigma'_x)\}_I^2 - (2\epsilon_0\epsilon_e - \epsilon_\delta)\{E_x/(1-\sigma'_x)\}_{II}^2] \quad \text{B(7)}$$

Acknowledgements

The authors are indebted to Dr. G. Paillotin for valuable comments and insight by suggesting the introduction of the parameter ν which results in the analytical expressions used in the text. We thank the Science Research Council for financial support.

References

1 Barber, J. and Mills, J.D. (1976) FEBS Lett. 68, 288—292
2 Barber, J. and Mills, J.D. and Love, A. (1977) FEBS Lett. 74, 174—181
3 Mills, J.D. and Barber, J. (1975) Arch. Biochem. Biophys. 170, 306—314
4 Nakatani, H.Y., Barber, J. and Forrester, J.A. (1978) Biochim. Biophys. Acta 504, 215—225
5 Gross, E.L. and Prasher, S.H. (1974) Arch. Biochem. Biophys. 164, 460—468
6 Barber, J. (1979) in Chlorophyll Organisation and Energy Transfer in Photosynthesis, Ciba Found. Symp. No. 61 (new series), pp. 283—304, Elsevier/Excerpta Medica, Amsterdam
7 Walz, D., Schuldiner, S. and Avron, M. (1971) Eur. J. Biochem. 22, 439—444
8 Jagendorf, A.T. and Smith, M. (1962) Plant Physiol. 37, 135—141
9 Telfer, A., Barber, J. and Jagendorf, A.T. (1980) Biochim. Biophys. Acta 591, 331—345
10 Nakatani, H.Y., Barber, J. and Minski, M.J. (1979) Biochim. Biophys. Acta 545, 24—35
11 Searle, G.W.F., Barber, J. and Mills, J.D. (1977) Biochim. Biophys. Acta 461, 413—425
12 Barber, J. and Searle, G.F.W. (1978) FEBS Lett. 92, 5—8
13 Barber, J. and Chow, W.S. (1979) FEBS Lett. 105, 5—10
14 Mills, J.D. and Barber, J. (1978) Biophys. J. 21, 257—272
15 Grahame, D.C. (1953) J. Chem. Phys. 21, 1054—1064
16 Verwey, E.J.W. and Overbeek, J.T.G. (1948) Theory of the Stability of Lyophobic Colloids, Elsevier, Amsterdam
17 Ninham, B.W. and Parsegian, V.A. (1971) J. Theor. Biol. 31, 405—428
18 Duniec, J.T., Sculley, M.J. and Thorne, S.W. (1979) J. Theor. Biol. 74, 473—484
19 Chow, W.S., Thorne, S.W., Duniec, J.T., Sculley, M.J. and Boardman, N.K. (1980) Arch. Biochem. Biophys., in the press
20 Overbeek, J.T.G. (1976) J. Colloid Interface Sci. 58, 408—422
21 Barber, J., Chow, W.S., Schoufflair, C. and Lannoye, R. (1980) Biochim. Biophys. Acta 591, 92—103
22 Mills, J.D. (1976) Ph.D. Thesis, University of London
23 Verwey, E.J.W. and Overbeek, J.T.G. (1948) Theory of the Stability of Lyophobic Colloids, pp. 92—94, Elsevier, Amsterdam
24 Sanfeld, A. (1968) in Monographs in Statistical Physics and Thermodynamics (Prigogine, I., ed.), Vol. 10, pp. 179—186, John Wiley, London